

Two-electronic component behavior in the multiband $\text{FeSe}_{0.42}\text{Te}_{0.58}$ superconductor

D. Arčon,^{1,2,*} P. Jeglič,¹ A. Zorko,¹ A. Potočnik,¹ A. Y. Ganin,³ Y. Takabayashi,⁴ M. J. Rosseinsky,³ and K. Prassides⁴

¹*Institute "Jozef Stefan", Jamova 39, 1000 Ljubljana, Slovenia*

²*Faculty of Mathematics and Physics, University of Ljubljana, Jadranska 19, 1000 Ljubljana, Slovenia*

³*Department of Chemistry, University of Liverpool, Liverpool L69 7ZD, UK*

⁴*Department of Chemistry, Durham University, Durham DH1 3LE, UK*

(Dated: December 6, 2013)

We report X-band EPR and ^{125}Te and ^{77}Se NMR measurements on single-crystalline superconducting $\text{FeSe}_{0.42}\text{Te}_{0.58}$ ($T_c = 11.5(1)$ K). The data provide evidence for the coexistence of intrinsic localized and itinerant electronic states. In the normal state, localized moments couple to itinerant electrons in the $\text{Fe}(\text{Se},\text{Te})$ layers and affect the local spin susceptibility and spin fluctuations. Below T_c , spin fluctuations become rapidly suppressed and an unconventional superconducting state emerges in which $1/T_1$ is reduced at a much faster rate than expected for conventional s - or s_{\pm} -wave symmetry. We suggest that the localized states arise from the strong electronic correlations within one of the Fe-derived bands. The multiband electronic structure together with the electronic correlations thus determine the normal and superconducting states of the $\text{FeSe}_{1-x}\text{Te}_x$ family, which appears much closer to other high- T_c superconductors than previously anticipated.

PACS numbers: 74.25.nj, 74.70.Xa

The competition between magnetism and superconductivity (SC) is a common theme in all high- T_c superconductors. In cuprates¹ and fullerenes,^{2,3} the parent compounds are antiferromagnetic (AF) Mott insulators and SC appears after doping with charge carriers or upon applying high pressure. Strong electron correlations are the driving force in these transitions. On the other hand, in iron-based superconductors their role in SC is less clear. They are believed to be weaker⁴ because the ground state of the parent compounds is metallic and a low-temperature spin density wave (SDW) instability is induced by the Fermi surface nesting. Iron-based superconductors have a complicated multiband structure with all five Fe d -bands crossing the Fermi level. It has been proposed that differences in the $p-d$ hybridization may lead to the formation of more localized orbitals.⁵ Therefore, each band could be affected by electron correlations differently to a degree that an orbital-selective Mott transition may take place.⁶

In order to address the problem of electronic correlations and possible charge localization, we focus on the $\text{FeSe}_{0.42}\text{Te}_{0.58}$ compound, a member of the layered iron-chalcogenide, FeQ ($Q = \text{Se}, \text{Te}$) superconductors. The two end members, $\text{Fe}_{1.01}\text{Se}$ and $\text{Fe}_{1+\delta}\text{Te}$ ($\delta \leq 0.14$), exhibit fundamentally different ambient-pressure ground states. $\text{Fe}_{1+\delta}\text{Se}$ is a superconductor with critical temperature $T_c \sim 9$ K at ambient pressure.⁷⁻⁹ On the other hand, AF long-range order develops in $\text{Fe}_{1+\delta}\text{Te}$ below ~ 65 K.¹⁰ The magnetic order vector $Q_{AF} = (\frac{1}{2}, \frac{1}{2})$, the rather large ordered moment exceeding $2 \mu_B/\text{Fe}$ and the Curie-Weiss-like susceptibility in the paramagnetic state of $\text{Fe}_{1+\delta}\text{Te}$ ¹¹ suggest that the magnetism is of a local-moment origin in contrast to the SDW phase found in other Fe-based superconductors. Moreover, inelastic neutron scattering measurements indicate a spin fluctuation spectrum, which is best described with an identical

model to that used for the normal-state spin excitations in the high- T_c cuprates.¹² In addition, an anomalously large mass renormalization, $m^*/m_{band} \approx 6-20$ has been reported recently for $\text{FeSe}_{0.42}\text{Te}_{0.58}$ from ARPES data,¹³ consistent with the high bulk specific heat coefficient, $\gamma = 39$ mJ/mol K².¹⁴ These results highlight the importance of electronic correlations in the FeQ family, which in analogy to other strongly correlated multiband systems may dramatically lower the energy difference between the coherent quasiparticle states and the incoherent excitations with more local character.¹³

Here we report a combined EPR and ^{77}Se , ^{125}Te NMR study of the $\text{FeSe}_{0.42}\text{Te}_{0.58}$ superconductor ($T_c = 11.5(1)$ K), which provide evidence for the coexistence of two electronic components arising from itinerant and localized states. The coupling between these states at the atomic scale leads to the screening of localized moments, suppression of the AF spin fluctuations and thus opens the possibility for the emergence of unconventional superconductivity. The intrinsic localized states are likely signatures of strong electron correlations making the FeQ family a close relative to other high- T_c superconductors.

The single-crystalline $\text{FeSe}_{0.42}\text{Te}_{0.58}$ sample used in this work was identical to that of ref. 13. Hexagonal FeSe (1.27(2)%) and elemental Se (2.31(4)%) were identified as impurities in crushed powders by synchrotron XRD measurements. The bulk magnetic susceptibility, χ_S , was measured with a commercial Quantum Design MPMS system on a 0.547 mg single crystal and with the magnetic field applied along the crystal c -axis. χ_S was determined by taking the difference between measurements performed in 3 and 2 T in order to subtract the contribution from ferromagnetic impurities. NMR frequency-swept spectra were measured in a magnetic field of 9.4 T with a two-pulse sequence $\beta - \tau - 2\beta - \tau - \text{echo}$, a pulse length $\tau_B = 4 \mu\text{s}$ and interpulse delay $\tau = 60 \mu\text{s}$. For

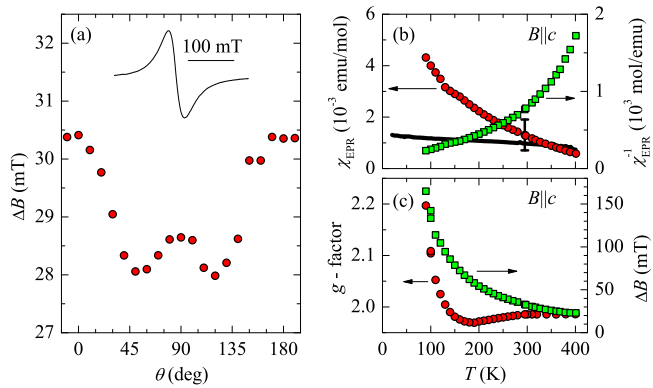


FIG. 1. (a) Angular dependence of the room temperature EPR linewidth in $\text{FeSe}_{0.42}\text{Te}_{0.58}$ single crystal. $\theta = 0$ is the $B||c$ crystal orientation. Inset: Room temperature EPR spectrum for $B||c$. Horizontal bar indicates field scale. (b) Temperature dependence of the EPR spin susceptibility, χ_{EPR} (circles, left scale), the bulk spin susceptibility, χ_S (black solid line) and the inverse spin susceptibility, χ_{EPR}^{-1} (squares, right scale). (c) Temperature dependence of the EPR g -factor (left scale, circles) and linewidth, ΔB (right scale, squares).

the temperature dependent X-band (9.6 GHz) cw-EPR experiments, a small piece of the crystal was exfoliated from the large crystal and sealed under dynamic vacuum in a 4-mm-diameter silica tube.

The very intense EPR resonance (inset Fig. 1a) has been measured at room temperature and is best described by Dyson lineshape as expected for metallic samples. At 300 K, the calibrated EPR intensity corresponds to a spin susceptibility, $\chi_{EPR} = 1.3(5) \times 10^{-3}$ emu/mol - the large uncertainty in the value of χ_{EPR} arises from difficulties in the precise positioning of the tiny single crystal in the resonator - which is comparable to the measured $\chi_S = 1.0(1) \times 10^{-3}$ emu/mol (Fig. 1b) and to that reported for $\text{FeTe}_{0.55}\text{Se}_{0.45}$.¹⁴ The negligibly small refined content of Fe interstitials between the Fe(Se/Te) slabs¹³ cannot be responsible for the measured χ_{EPR} . On the other hand, hexagonal FeSe_{1-x} phases can be ferromagnetic with Curie temperatures exceeding room temperature¹⁵ and could give rise to strong ferromagnetic resonance. However, since the hexagonal FeSe_{1-x} magnetization is already fully saturated in the field of the EPR resonance (~ 0.33 T), it cannot account for the strong temperature dependence of χ_{EPR} (Fig. 1b). We thus conclude that the measured EPR signal is *intrinsic*.

The EPR resonance shows a strong angular dependence of the EPR linewidth, ΔB , with a minimum value at the angle $\theta_m = 54^\circ$ when the crystal is rotated away from the $B||c$ -orientation (Fig. 1a). The minimum in ΔB can be reproduced with the dipolar interactions between the exchange coupled localized moments centered at Fe-positions in the $\text{FeSe}_{0.42}\text{Te}_{0.58}$ structure. This implies that states with more local character may also exist in addition to the quasiparticle states. These are further evidenced by the temperature dependence of χ_{EPR} , which rapidly increases with decreasing temperature (Fig. 1b).

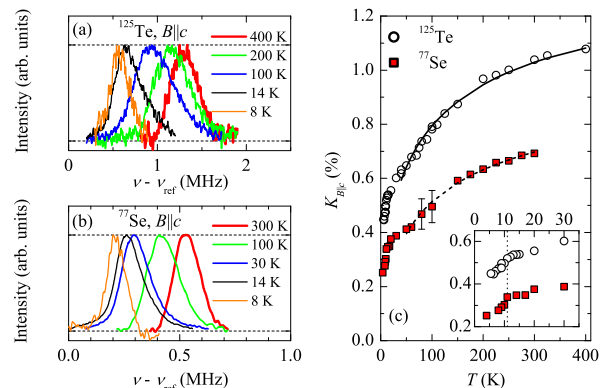


FIG. 2. Frequency-swept (a) ^{125}Te and (b) ^{77}Se NMR spectra of $\text{FeSe}_{0.42}\text{Te}_{0.58}$ single crystal measured with $B||c$. (c) Temperature dependence of the ^{125}Te (^{125}K , open circles) and ^{77}Se (^{77}K , solid squares) Knight shifts. The lines are fits to the model described in the text. Inset: expanded region near $T_c = 11.5(1)$ K, showing the clear drop of ^{125}K and ^{77}K .

However, the non-linear dependence of the inverse EPR susceptibility between 100 and 400 K (Fig. 1b) is not consistent with the simple Curie-Weiss law expected for localized moments only, meaning that the measured EPR signal has contributions from both quasiparticle and localised states. Simple macroscopic phase segregation into metallic and insulating fractions would have implied that χ_{EPR} can be expressed as $\chi_{EPR} = \chi_c + \chi_l$, where χ_c is the spin susceptibility of quasiparticles, which is expected to be only weakly temperature dependent and χ_l is the spin susceptibility of localized states. But this approach results in unphysical parameters (negative χ_c), thus leading to the conclusion that both electronic components not only coexist at the nanometric or atomic scale but that they are also strongly coupled. Such coupling could be responsible for the rapid increase in ΔB and g -factor with decreasing temperature (Fig. 1c), which indicates development of local magnetic fields sensed by these states. It could also account for another surprising observation: namely, $\chi_{EPR}(T)$ is larger than the weakly temperature-dependent χ_S below room temperature (Fig. 1b). If the coupling is strong enough, then localized states polarize conduction electrons and reduce the effective moment measured in bulk experiments.

To confirm these hypotheses, we employed the NMR local probe technique, which can provide insight on the coexisting electronic components at different scales. In addition, it is not sensitive to impurities in the $\sim 1\%$ range. Figs. 2a,b show the ^{125}Te and ^{77}Se NMR spectra recorded for $B||c$. The room temperature linewidths of ^{125}Te and ^{77}Se resonances, $\delta^{125}\nu_{1/2} \approx 420$ kHz and $\delta^{77}\nu_{1/2} \approx 130$ kHz, respectively, imply that the local-site structural inhomogeneities resulting from the statistical Se/Te site occupation slightly broaden the ^{125}Te and ^{77}Se NMR spectra, e.g. with respect to the ^{77}Se NMR linewidth measured for $\text{Fe}_{1.01}\text{Se}$.¹⁶ For comparison, $\delta^{77}\nu_{1/2}$ is similar to those in $\text{Fe}_{1.04}\text{Se}_{0.33}\text{Te}_{0.67}$.¹⁷

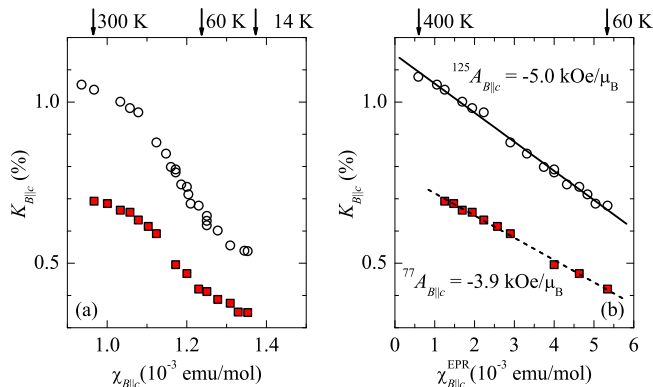


FIG. 3. ^{125}K and ^{77}K Knight shifts versus (a) bulk susceptibility, $\chi_{B||c}$ and (b) χ_{EPR} with temperature as an implicit parameter.

or $\text{FeSe}_{0.92}$.¹⁸ Interestingly, the ratio, $\delta^{125}\nu_{1/2}/\delta^{77}\nu_{1/2} \approx 3.2$ is significantly larger than that of the corresponding gyromagnetic ratios, $^{125}\gamma/^{77}\gamma = 1.65$, which is consistent with differences in the $p-d$ hybridization between FeTe and FeSe .²⁰

The room temperature NMR spectra are strongly shifted to higher frequencies with respect to the reference. The Knight shifts are $^{125}\text{K} = 1.038(2)\%$ and $^{77}\text{K} = 0.692(2)\%$ for ^{125}Te and ^{77}Se nuclei, respectively. The resonances shift considerably to lower frequencies with decreasing temperature (Fig. 2c): $\Delta^{125}\text{K} = -0.524\%$ and $\Delta^{77}\text{K} = -0.316\%$ between 300 and 20 K. A similar decrease of ^{77}K has been reported for $\text{Fe}_{1.01}\text{Se}$ and $\text{Fe}_{1.04}\text{Se}_{0.33}\text{Te}_{0.67}$.¹⁶⁻¹⁸ However, the Knight shifts, ${}^n\text{K}$ ($n = 77, 125$) do not scale with the bulk spin susceptibility over the entire temperature range (Fig. 3a). NMR data thus provide direct evidence that the local and bulk spin susceptibilities are different in the investigated sample. On the other hand, comparing ${}^n\text{K}$ with χ_{EPR} , which also measures the local spin susceptibility, reveals excellent linear scaling (Fig. 3b). If we express the temperature-dependent spin part of the Knight shift as ${}^n\text{K}(T) = \frac{{}^n A_{B||c}}{N_A \mu_B} \chi_{EPR}$, we derive the coupling constants, $^{125}A_{B||c} = -5.0(5) \text{ kOe}/\mu_B$ and $^{77}A_{B||c} = -3.9(8) \text{ kOe}/\mu_B$. Since we scale ${}^n\text{K}$ with the local rather than the bulk spin susceptibility, the coupling constants are different from those extracted for $\text{Fe}_{1.04}\text{Se}_{0.33}\text{Te}_{0.67}$ only from low temperature ($< 100 \text{ K}$) data.¹⁷

The scaling of ${}^n\text{K}$ with the local rather than with the bulk spin susceptibility is a strong indication for the coexistence of coupled localized and itinerant states at the atomic scale. In the case of two coupled spin components, there are generally three contributions to the spin part of the Knight shift, ${}^n\text{K}_S = {}^n\text{K}_c + {}^n\text{K}_l + {}^n\text{K}_{ex}$. Here ${}^n\text{K}_c$ stands for the coupling of Te/Se nuclei to the itinerant electrons via hyperfine coupling interaction and should be only weakly temperature dependent, ${}^n\text{K}_l$ describes the interaction with the localized states, and ${}^n\text{K}_{ex}$ is the additional Knight shift arising from the spin-density polarization due to the interaction between the localized

and itinerant states. ${}^n\text{K}_{ex}$ should be negative in sign,²¹ as it is indeed observed. It is intriguing that the strong temperature dependence of ${}^n\text{K}$ can be simulated with the expression ${}^n\text{K} \propto (1 - (T/T^*)) \log(T^*/T)$, which has been applied to a number of Kondo lattice materials.²² Here T^* is the correlated Kondo temperature and is a measure of the intersite localized state interactions.²² Excellent agreement with the experimental data for both nuclei (Fig. 2b) is obtained with the same $T^* \sim 800 \text{ K}$, which falls within the 50-80 meV range of the crossover energy between quasiparticle states and excitations with local character.¹³

The most important experimental finding of this work is that in $\text{FeSe}_{0.42}\text{Te}_{0.58}$ intrinsic states with localized character may form, coexist and couple with itinerant states. The coupling between the two electronic components governs the normal as well as the superconducting properties. It is suggested that in such strongly correlated systems this coupling plays a vital role in suppressing magnetism and promoting high-temperature superconductivity.²³ Therefore, in order to test the suppression of spin fluctuations we turn to the spin-lattice relaxation time, nT_1 data. Fig. 4a shows the frequency dependence of $1/{}^{77}T_1T$ for ^{77}Se NMR spectra at selected temperatures. It is evident that $1/{}^{77}T_1T$ substantially varies over the ^{77}Se NMR line and the ratio between largest and shortest $1/{}^{77}T_1T$ measured for the low- and high-frequency spectral shoulders can be as large as 4 (at 50 K). Therefore, a simple two relaxation-times model earlier applied^{17,18} to $\text{FeSe}_{0.92}$ and $\text{Fe}_{1.04}\text{Se}_{0.33}\text{Te}_{0.67}$ oversimplifies the experimental situation and may even lead to erroneous conclusions. All $1/{}^{77}T_1T$ values fall on nearly the same universal Knight shift-dependent curve described by the Korringa relation, ${}^{77}T_1T{}^{77}K_S^2 = \frac{\hbar}{4\pi k_B} \frac{\gamma_e^2}{\gamma_{Se}} \beta$. Here γ_e and γ_{Se} are the electron and nuclear gyromagnetic ratios and ${}^{77}K_S$ is obtained from ${}^{77}K_S = {}^{77}K - {}^{77}K_{orb}$, where ${}^{77}K_{orb} = 0.24(3)\%$ is a temperature-independent orbital shift. Deviations from this universal dependence, mostly visible at high temperatures, indicate the presence of another weaker relaxation channel, for which ${}^{77}T_1^{-1} = \text{const.}$ might suggest relaxation via localized moments. A phenomenological parameter, β characterizes the extent of spin fluctuations and has been recently studied in the context of the normal state properties of iron-based superconductors.¹⁹ Since we obtain $\beta = 1.0(1)$, we conclude that AF spin fluctuations are not strongly enhanced. Another indication for this comes from the validity of Korringa relation over a broad temperature interval (Fig. 4b). This is in striking contrast to FeSe , which clearly shows enhancement of AF spin fluctuations towards T_c .¹⁶ Apparently these spin fluctuations become strongly suppressed upon Te substitution and are only visible again after the application of pressure.²⁴ This is fully consistent with the present picture of localized states. Namely high T^* suggests strong local Kondo effects where local magnetic moments become screened and unconventional supercon-

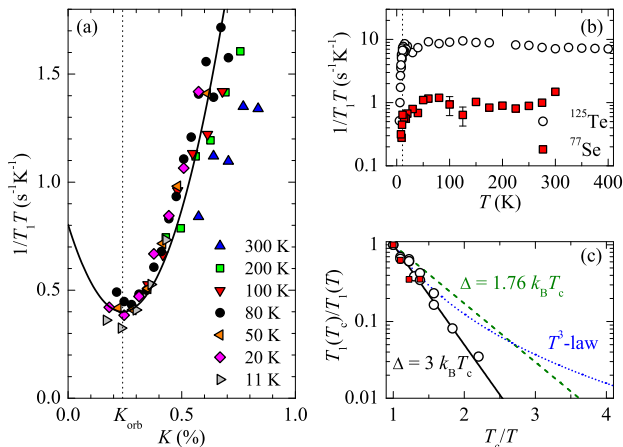


FIG. 4. (a) Frequency dependence of $1/^{77}\text{T}_1T$ measured at various temperatures (bottom). All measurements fall on the same curve, which scales as $(^{77}K - ^{77}K_{orb})^2$ with $^{77}K_{orb} = 0.24(3)\%$ (solid line). (b) Temperature dependence of ^{125}Te (open circles) and ^{77}Se (solid squares) $1/^{n}\text{T}_1T$ rates. (c) Temperature dependence of $T_1(T_c)/T_1(T)$ below $T_c = 11.5(1)$ K. The rate of suppression of $1/T_1$ below T_c is significantly larger than expected for BCS-type superconductivity.

ductivity may develop instead of magnetism.

Last, we turn to the ^{125}Te and ^{77}Se NMR data below $T_c = 11.5(1)$ K. The ^{125}Te resonance suddenly becomes narrower and more symmetric, while its intensity starts to decrease (Fig. 2a). The abrupt decrease in the signal intensity is due to the Meissner shielding of the rf pulses. On the other hand, the sudden decrease in the linewidth is more surprising. In the singlet superconducting state, we expect χ_S to vanish and therefore any broadening and extra resonance shift caused by the interaction between the localized and superconducting states should be reduced below T_c . ^{125}K and ^{77}K suddenly start to decrease at faster rate below T_c (inset Fig. 2b), thus indicating the vanishing spin susceptibility as expected both for s - and d -wave pairing. This is further supported by the $^{n}\text{T}_1$ data. $^{n}\text{T}_1^{-1}$ values are strongly reduced below T_c for both nuclei (Fig. 4c). We also note that $1/T_1$ does not show a coherence peak which has been also missing in FeSe^{16} and other Fe-based superconductors.^{18,25–27} $1/^{n}\text{T}_1$ is exponentially

suppressed below T_c with an effective gap, $\Delta = 3k_B T_c$ which is much larger than that predicted for conventional s -wave BCS-type pairing in the weak-coupling limit, $\Delta = 1.76k_B T_c$. Neither the low-temperature T^3 dependence (expected within the s_{\pm} gap scenario) nor the two-gap dependence is found down to $T_c/T = 2.25$, in striking contrast to reports for Fe-pnictide superconductors. We also stress that the obtained Δ is in excellent agreement with that found by point-contact Andreev reflection spectroscopy ($\Delta = 3.1k_B T_c$)²⁸ and implies a single s -wave order parameter in the strong coupling limit. An alternative explanation would be in terms of considerable anisotropy of the superconducting gap frequently noticed in systems with strong electronic correlations.²⁹ Additional experiments are needed to verify this scenario.

The detection of intrinsic localized moments coupled to itinerant electrons and leading to unconventional SC shows some similarities with strongly correlated electron systems. The question to resolve is, how these localized states form in $\text{FeSe}_{0.42}\text{Te}_{0.58}$. Orbitally selective Mott localization has been recently proposed⁶ for Fe-based superconductors. This model could well explain the strong local moment screening and suppression of AF fluctuations in the normal state as well as the ^{125}Te and ^{77}Se NMR data below T_c . The coexisting magnetic and superconducting order parameters on the atomic scale that have been recently suggested for FeSe from μSR experiments³⁰ is also consistent with this picture. All these results point to the importance of strong intraband electronic correlations which may explain the rapid suppression of $1/T_1$ below T_c , the strong sensitivity of $\text{FeSe}_{1-x}\text{Te}_x$ superconductivity both to chemical substitution and applied pressure^{31–34} and the induced static magnetic order at pressures exceeding 1 GPa.³⁰

In conclusion, we have carried out EPR and NMR studies of $\text{FeSe}_{0.42}\text{Te}_{0.58}$ single crystal. We found the presence of intrinsic localized states coupled to quasiparticles. The screening of these states suppresses the AF spin fluctuations and thus opens the possibility for the emergence of unconventional superconductivity. Although the exact origin of localized states should be investigated in the future, the present picture is consistent with the intraband electronic correlations leading to a localization of one of the Fe-derived bands. In this respect, the FeQ family appears to be much closer to other high- T_c superconductors and should be treated on a similar footing.

* denis.arcon@ijs.si

¹ P.A. Lee et al., *Rev. Mod. Phys.* **78**, 17 (2006).
² Y. Takabayashi et al., *Science* **323**, 1585 (2009).
³ A. Y. Ganin et al., *Nature*, doi:10.1038/nature09120.
⁴ W.L. Yang et al., *Phys. Rev. B* **80**, 014508 (2009).
⁵ J. Wu et al., *Phys. Rev. Lett.* **101**, 126401 (2008).
⁶ L. de' Medici et al., *J. Supercond. Novel Magn.* **22**, 535 (2009).

⁷ F.C. Hsu et al., *Proc. Natl. Acad. Sci.* **105**, 14262 (2008).
⁸ S. Margadonna et al., *Chem. Commun.* 5607 (2008).
⁹ T.M. McQueen et al., *Phys. Rev. B* **79**, 014522 (2009).
¹⁰ Y. Xia et al., *Phys. Rev. Lett.* **103**, 037002 (2009).
¹¹ S. Li et al., *Phys. Rev. B* **79**, 054503 (2009).
¹² M.D. Lumsden et al., *Nat. Phys.* **6**, 182 (2010).
¹³ A. Tamai et al., *Phys. Rev. Lett.* **104**, 097002 (2010).
¹⁴ B. C. Sales, et al. *Phys. Rev. B* **79**, 094521 (2009).

- ¹⁵ T. Kamimura and T. Iwata, *J. Phys. Soc. Jpn.* **45** 1769 (1978).
- ¹⁶ T. Imai et al., *Phys. Rev. Lett.* **102**, 177005 (2009).
- ¹⁷ C. Michioka et al., arXiv:0911.3729.
- ¹⁸ H. Kotegawa et al., *J. Phys. Soc. Jpn.* **77**, 113703 (2008).
- ¹⁹ P. Jeglič et al., *Phys. Rev. B* **81**, 140511(R) (2010).
- ²⁰ T. Miyake et al., *J. Phys. Soc. Jpn.* **79**, 044705 (2010).
- ²¹ J.B. Boyce and C.P. Slichter, *Phys. Rev. B* **13**, 379 (1976).
- ²² N.J. Curro et al., *Phys. Rev. B* **70**, 235117 (2004).
- ²³ F. J. Ohkawa, *J. Phys. Soc. Jpn* **61**, 4490 (1992).
- ²⁴ Y. Shimizu et al., *J. Phys. Soc. Jpn.* **78**, 123709 (2009).
- ²⁵ H.-J. Grafe et al., *New. J. Phys.* **11**, 035002 (2009).
- ²⁶ F.L. Ning et al., *J. Phys. Soc. Jpn* **77**, 103705 (2008).
- ²⁷ Y. Nakai et al., *J. Phys. Soc. Jpn* **77**, 073701(2008).
- ²⁸ W.K. Park et al., arXiv:1005.0190.
- ²⁹ D.F. Smith and C.P. Slichter, *Lect. Notes Phys.* **684**, 243 (2006).
- ³⁰ M. Bendele et al., *Phys. Rev. Lett.* **104**, 087003 (2010).
- ³¹ S. Margadonna et al., *Phys. Rev. B* **80**, 064506 (2009).
- ³² S. Medvedev et al., *Nature Mater.* **8**, 630 (2009).
- ³³ Y. Mizuguchi et al., *Appl. Phys. Lett.* **94**, 012503 (2009).
- ³⁴ N.C. Gresty et al., *J. Am. Chem. Soc.* **131**, 16944 (2009).